PURDUE UNIVERSITY

Weldon School of Biomedical Engineering

The Convergence of Differences, The Future of Excellence

Development of Non-Invasive *In Vivo* Ultrasound Imaging Techniques for Elastase-Induced Experimental Abdominal Aortic Aneurysms

Alexa A. Yrineo, Elizabeth A. Nunamaker, Hilary D. Schroeder, Amy E. Bogucki, Craig J. Goergen

The Purdue Cardiovascular Imaging Research Laboratory in West Lafayette, Indiana

Introduction and Objectives

- Abdominal aortic aneurysms (AAAs) are pathological dilations of the aorta which are associated with significant morbidity and mortality due to rupture.
- Aneurysms are clinically defined as an aortic diameter 50% larger than normal.
- Risk factors include hypertension, increased age and male gender.
- The underlying mechanisms that cause this inflammatory disease are not fully understood.
- Rodent models that mimic the human condition have been developed to provide insight into disease pathogenesis.
- Elastase has been determined to play a major role in the destruction of elastin within the aortic wall [1].
- Objective: Use high-frequency ultrasound to track elastase-induced AAA progression in rats.

Materials and Methods

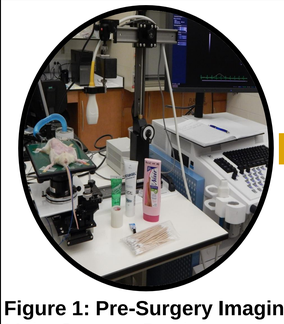

Figure 1: Pre-Surgery Imaging Male, Sprague Dawley rats (n=8; 10 weeks old; 298 ± 10 g) were imaged with a VisualSonics Vevo 2100 ultrasound. Anesthesia: 2% isoflurane in 1.5 L/min O_2 . Hair was removed with depilatory cream and heart rate and body temperature were monitored.

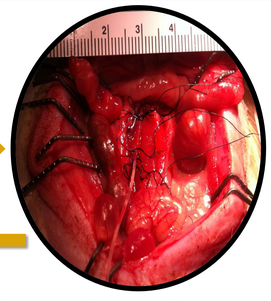

Figure 2: Surgical Procedure Temporary ligatures were placed around proximal and distal sections of the infrarenal aorta and a PE-10 catheter was inserted through an aortotomy above the trifurcation to infuse porcine pancreatic elastase (0.44 U; 30 min) [2].

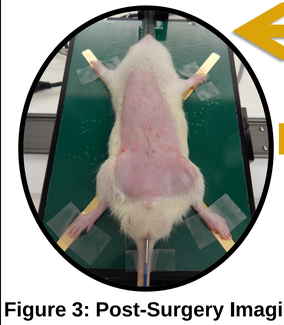

Figure 3: Post-Surgery Imaging Rats were imaged on days 3, 7, 14, 21, and 28. In the transverse plane, B-Mode, M-Mode, Color Doppler, Power Doppler, and 3D images were acquired. In the longitudinal plane, images were collected in B-Mode, M-Mode, Color Doppler, Power Doppler, and Pulsed Wave Doppler.

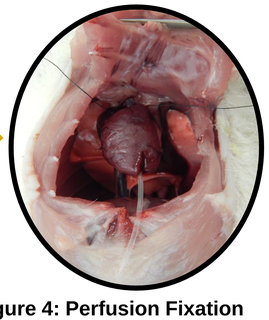

Figure 4: Perfusion Fixation Rats were sacrificed on day 29. A catheter was inserted into the aorta through an incision in the left ventricle. Saline (0.9% NaCl; 50 mL) was perfused followed by PFA (4%; 10 mL) and agarose (1% low melt; 10 mL). After 10 min. on ice, the heart, aorta and kidneys were dissected.

Results

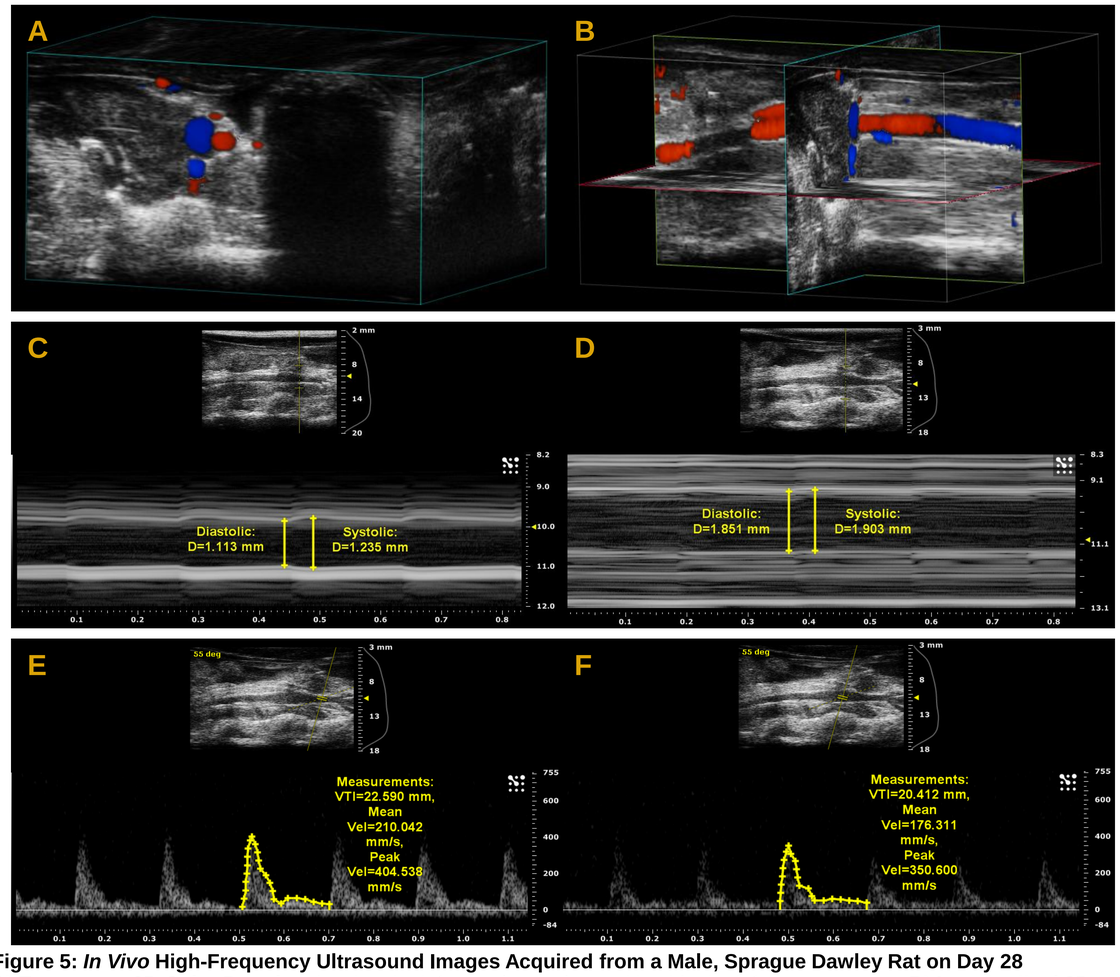

Figure 5: *In Vivo* High-Frequency Ultrasound Images Acquired from a Male, Sprague Dawley Rat on Day 28 **A) Transverse 3D Color Doppler** showing the infrarenal aorta located beside the inferior vena cava. **B) Longitudinal 3D Color Doppler** providing visualization of aortic blood flow. Red indicates flow towards the transducer and blue away. **C) Longitudinal M-Mode** of a healthy section of the aorta showing the pulsatile motion of the vessel walls compared to the **D) Longitudinal M-Mode** of an aneurysmal section showing increased vessel stiffness. **E) Longitudinal Pulsed Wave Doppler** depicting the velocity profile inside a healthy section of the aorta compared to the **F) Longitudinal Pulsed Wave Doppler** inside an aneurysmal section.

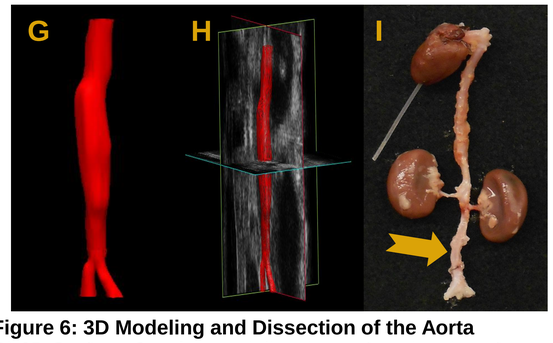

Figure 6: 3D Modeling and Dissection of the Aorta **G) 3D Surface Overlay** modeling the perfused region of the infrarenal aorta after 21 days. The expansion of the vessel is visible above the bifurcation in the **H) 3D Data Overlay. I) Dissection of the Aorta** attached to the heart and kidneys on day 29 reveals the ex vivo aneurysmal section below the renal arteries and above the aortotomy created during surgery.

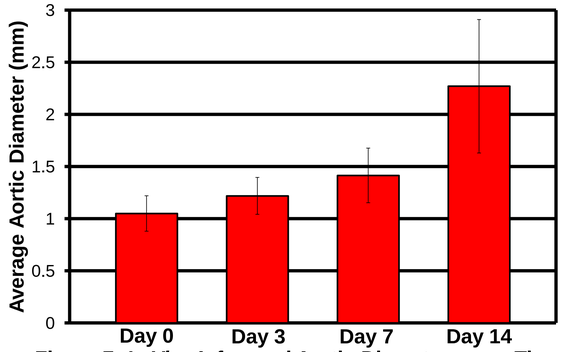

Figure 7: *In Vivo* Infrarenal Aortic Diameters over Time The longitudinal diameters are displayed as average ± standard deviation (n=4). The measurements were taken from the outermost walls of the aorta in the acquired B-Mode images. Prior to surgery the aorta had a diameter of 1.05 ± 0.17 mm and 14 days after surgery the aorta measured 2.27 ± 0.64 mm.

Discussion and Conclusions

- Of the 8 rats used in this study, 4 survived for 28 days.
- The infrarenal aortas of the male, Sprague Dawley rats expanded to a diameter 100% larger than normal after just 14 days (Figure 7).
- Prior to surgery the Green-Lagrange strain on the healthy vessel was 0.21 ± 0.09 and 14 days after surgery the strain on the aneurysmal vessel was 0.11 ± 0.07 (n=4; Figure 5; C and D).
- Mean velocity measured 324 ± 31 mm/s on day 0 and 239 ± 39 mm/s on day 14 (n=4; Figure 5; E and F).
- The perfused region is clinically relevant due its location below the renal arteries. These AAAs are fusiform in shape rather than saccular (Figure 6; G).
- Conclusion: Utilizing high-frequency ultrasound to characterize elastase-induced rat AAA progression increases our understanding of aneurysm pathogenesis.

Future Work

- Dr. Michael Murphy and his group have tested the hypothesis that IL-17 produced by CD4+ T-cells modulates inflammation, leading to the pathogenesis of AAA [3].
- The results demonstrated that immunomodulation of IL-17 by mesenchymal stem cells can offer protection against aneurysm formation [3].
- Our efforts using this elastase-induced AAA rat model will benefit future mesenchymal stem cell work aimed at preventing aneurysm formation by modulating the immune response.
- We plan to inject mesenchymal stem cells from placenta, adipose tissue and bone marrow into rats via the tail vein.

Acknowledgements

Thank you to Drs. Elizabeth Nunamaker and Gary Lantz for their surgical expertise. Also, thank you to Dr. Craig Goergen and the SURF program for this opportunity.

SURF 2013

References

[1] S. Anidjar, J.-L. Salzmann, D. Gentric, P. Lagneau, J.-P. Camilleri, and J.-B. Michel, "Elastase-Induced Experimental Aneurysms in Rats," *Circulation,* vol. 82, pp. 973-81, 1990.

[2] J. Azuma, T. Asagami, R. Dalman, and P. Tsao, "Creation of Murine Experimental Abdominal Aortic Aneurysms with Elastase," *Journal of Visualized Experiments,* vol. 29, 2009.

[3] Sharma, A.K., et al., *Experimental abdominal aortic aneurysm formation is mediated by IL-17 and attenuated by mesenchymal stem cell treatment.* Circulation, 2012. 126(11 Suppl 1): p. S38-45.